### Title

Tunable Properties of Poly-DL-Lactide-Monomethoxypolyethylene Glycol Porous Microparticles for Sustained Release of Polyethylenimine-DNA Polyplexes




### Journal

AAPS PharmSciTech, 20(1)

### ISSN

1530-9932



### Authors

Terry, Treniece L
Givens, Brittany E
Rodgers, Victor GJ
et al.



### Publication Date

2019

### DOI

10.1208/s12249-018-1215-9

Peer reviewed

*AAPS PharmSciTech* (2019) 20:23
DOI: 10.1208/s12249-018-1215-9

*Research Article*

*Theme: Translational Multi-Disciplinary Approach for the Drug and Gene Delivery Systems*
*Guest Editors: Mahavir Bhupal Chougule, Vijaykumar B. Sutariya and Sudip K. Das*

# Tunable Properties of Poly-DL-Lactide-Monomethoxypolyethylene Glycol Porous Microparticles for Sustained Release of Polyethylenimine-DNA Polyplexes

**Treniece L. Terry,[1,2] Brittany E. Givens,[1,2] Victor G. J. Rodgers,[3] and Aliasger K. Salem[1,2,4]**

*Received 23 July 2018; accepted 8 October 2018*

***Abstract.*** Direct pulmonary delivery is a promising step in developing effective gene therapies for respiratory disease. Gene therapies can be used to treat the root cause of diseases, rather than just the symptoms. However, developing effective therapies that do not cause toxicity and that successfully reach the target site at therapeutic levels is challenging. We have developed a polymer-DNA complex utilizing polyethylene imine (PEI) and DNA, which was then encapsulated into poly(lactic acid)-*co*-monomethoxy poly(ethylene glycol) (PLA-mPEG) microparticles *via* double emulsion, solvent evaporation. Then, the resultant particle size, porosity, and encapsulation efficiency were measured as a function of altering preparation parameters. Microsphere formation was confirmed from scanning electron micrographs and the aerodynamic particle diameter was measured using an aerodynamic particle sizer. Several formulations produced particles with aerodynamic diameters in the 0–5 μm range despite having larger particle diameters which is indicative of porous particles. Furthermore, these aerodynamic diameters correspond to high deposition within the airways when inhaled and the measured DNA content indicated high encapsulation efficiency. Thus, this formulation provides promise for developing inhalable gene therapies.

**KEY WORDS:** PLA; PEG; polyplexes; microspheres.

## INTRODUCTION

Gene therapy is useful for treating the root cause of genetic diseases, rather than ephemerally mitigating the symptoms. Gene therapy has made significant headway in treating retinal diseases and thalassemia with the potential to treat even more diseases (1–3). In comparison, focus on mitigating symptoms is common in other chronic diseases such as cystic fibrosis and asthma (4–6). Existing inhalation therapies for genes and drugs have associated clinical challenges that still need addressing (1,7). For example, dry powder therapy is often utilized for delivery of genes and drugs directly to the lung (8,9), but the lung has numerous physiological barriers intended to prevent invasion by foreign pathogens or particulates, thus impeding successful particle delivery (7). Additionally, gene delivery requires that the foreign DNA is able to penetrate the nuclei of cells and integrate into the host DNA (7). Efficient aerosol delivery systems that consider the aerodynamic diameter of particles, and the amount of DNA deposited at the target site are critical to the development of effective approaches to gene delivery to the lung (10). Polymeric particles have gained interest as potential drug and gene delivery systems because they offer protection of the cargo from degradation, increase drug circulation time, can provide sustained release of the cargo over time, are highly tunable, and, in many cases, are biocompatible (11–19).

Polymer-DNA complexes (polyplexes) utilizing the cationic polymer polyethylene imine (PEI) have high transfection rates when delivered intravenously or intratracheally, but each method of delivery can induce toxicity (13,20). Thus, inhalation may be an alternative delivery method for DNA therapy (13). In fact, direct pulmonary delivery is advantageous because it is a non-invasive targeting method providing a high delivered dose to the target site

Guest Editors: Mahavir Bhupal Chougule, Vijaykumar B. Sutariya and Sudip K. Das

**Electronic supplementary material** The online version of this article (https://doi.org/10.1208/s12249-018-1215-9) contains supplementary material, which is available to authorized users.

[1] Department of Pharmaceutical Sciences and Experimental Therapeutics, College of Pharmacy, University of Iowa, 115 S. Grand Avenue, S228 PHAR, Iowa City, Iowa 52242, USA.
[2] Department of Chemical and Biochemical Engineering, College of Engineering, University of Iowa, 115 S. Grand Avenue, S228 PHAR, Iowa City, Iowa 52242, USA.
[3] Department of Bioengineering, University of California, Riverside, Riverside, California 92521, USA.
[4] To whom correspondence should be addressed. (e–mail: aliasger-salem@uiowa.edu)

Published online: 02 January 2019

and fewer adverse reactions compared with systemic delivery (21). When DNA is encapsulated within a polymeric particle, it is protected from enzymatic degradation which improves the likelihood of the DNA reaching the target cells, although it does not guarantee nuclear entry (15–19,22–26). At the appropriate ratio of nitrogens in the polymer and phosphates in the DNA (N:P ratio), PEI imparts polyplexes with a positive charge, which enhances the cellular uptake (22–24,27–29). Due to the air-blood barrier in the alveoli, the cargo contained within porous PLGA microparticles delivered *via* inhalation resulted in high systemic bioavailability (30). PEGylation of polymeric particles has also been shown to enhance pulmonary absorption and retention (11). Furthermore, inhaled therapies bypass first pass metabolism in the liver and do not require entry into the blood stream to access the lungs *via* systemic circulation (31). Several limitations must be considered when developing pharmaceutical agents for direct pulmonary delivery, most notably aerodynamic diameter and subsequent particle deposition. Particles that have an aerodynamic diameter of 1–3 μm have been demonstrated as optimal for deposition in the lower airways (30).

Direct pulmonary delivery *via* non-viral vectors, including polymeric particles, has reached the clinical trial stage for a number of drugs, genes, and diseases. Non-viral vectors are advantageous delivery systems because they are cheaper and often safer than attenuated viruses (3). Kamada currently has an International Phase II/III clinical trial for α1-antitrypsin to treat emphysema in seven countries (32). However, many drugs do not reach necessary therapeutic levels in clinical trials (33), whereas others, particularly Exubera®, have since been removed from the shelves for undisclosed reasons, highlighting a key drawback in the direct pulmonary delivery formulation world (11). Even so, PEI-DNA complexes are stable for aerosol delivery and successfully altered gene expression in murine lung (34). This points to a particularly promising method for gene therapy utilizing direct pulmonary delivery.

In the present work, we systematically altered preparation conditions to generate porous polymeric particles loaded with polyplexes as a model system for aerosolized gene delivery to the lungs. The particles were developed using a block co-polymer of poly(lactic acid) (PLA) and monomethoxy-poly(ethylene glycol) (mPEG) where the degree of porosity was controlled by altering the amount of organic solvents, surfactant, or water in the double emulsion. Particles were characterized according to the amount of DNA loaded, release kinetics of the DNA, surface morphology, and aerodynamic diameter. We discovered that changing the formulation parameters affected the average particle diameter, aerodynamic diameter, and the porosity without clearly altering encapsulation efficiency. These results provide insight into the means of tuning the properties of polymer particles for airway gene therapy applications. This knowledge has the potential to enable the development of more effective treatments for chronic respiratory disease.

## MATERIAL AND METHODS

### Materials

Poly(vinyl alcohol) (PVA, $M_w$ 30–70 kDa), 88% hydrolyzed and branched PEI ($M_w$ 25 kDa), DNA from herring sperm, sucrose, 2% osmium tetroxide, reagent grade dichloromethane (DCM), and ethyl acetate (EA) were purchased from Sigma Aldrich (St. Louis, MO). PLA was polymerized from DL-lactide monomers and mPEG ($M_w$ 4000) from Aldrich; mPEG was dried by azeotropic distillation with anhydrous toluene prior to use. Tin octoate ($Sn(Oct)_2$) was purchased from Aldrich and degassed for 10 min prior to use. Reagent grade ethyl ether was used without further purification. Phosphate-buffered saline (PBS) at pH 7.4 was purchased from Gibco (Waltham, MA).

### Synthesis of PEI-DNA Polyplexes

Branched PEI was weighed and suspended in distilled water to a final concentration of 1 mg/mL. Polyplexes were prepared by mixing the PEI solution, herring sperm DNA, and distilled water to obtain a mixture of 0.08 mg/mL DNA. Samples were vortexed for 30 s and allowed to sit at room temperature for DNA and PEI to complete complexation. Confirmation of this method was previously published for PLGA/PAMAM polyplexes (23).

### Polymerization of PLA and mPEG

Copolymers of PLA and mPEG were prepared using ring-opening polymerization co-initiated with $Sn(Oct)_2$ and mPEG (Fig. 1). Predetermined amounts of D,L-lactide monomers and the co-initiator mPEG at an 8:1 ratio were dissolved in anhydrous toluene at 25% (*w*/*w*) in a 250-mL round bottom flask with a silanized glass wall immersed in an oil bath at 120°C with mild stirring. A 5% *w*/*v* solution of $Sn(Oct)_2$ was added dropwise to form a 1% *w*/*v* solution in anhydrous toluene. Reactions proceeded for 4–6 h, until the solution became turbid. Polymers were purified *via* precipitation in chilled ethyl ether and the chemical structures were determined using proton $^1$H NMR (300 Hz, Bruker spectrophotometer Billerica, MA) with tetramethylsilane (TMS) as an internal reference for chemical shifts (ppm). The degree of polymerization, $\overline{DP}_{PLA}$, and the number average molecular weight, $M_n$, were calculated according to the following equations, respectively:

$$\overline{DP}_{PLA} = \overline{DP}_{PEG} \times \frac{{}^{LA}/_{EG}}{n_{LA}} \tag{1}$$

$$\overline{M}_n = n_{PEG} M_{n,PEG} + n_{LA} M_{w,LA} \overline{DP}_{PLA} \tag{2}$$

where $\overline{DP}_{PEG}$ is the degree of polymerization of *PLA*, *LA*/*EG* is the mass ratio of lactide (*LA*) to ethylene glycol (*EG*), $n_{LA}$ is the mass fraction of *LA*, $M_{n,\ PEG}$ is the number-average molecular weight of *PEG*, and $M_{w,\ LA}$ is the weight-average molecular weight of *LA*.

### Microparticle Formation

Porous polymeric particles encapsulating PEI-DNA complexes were prepared using a modified water in oil in water ($W_1/O/W_2$) double emulsion solvent evaporation

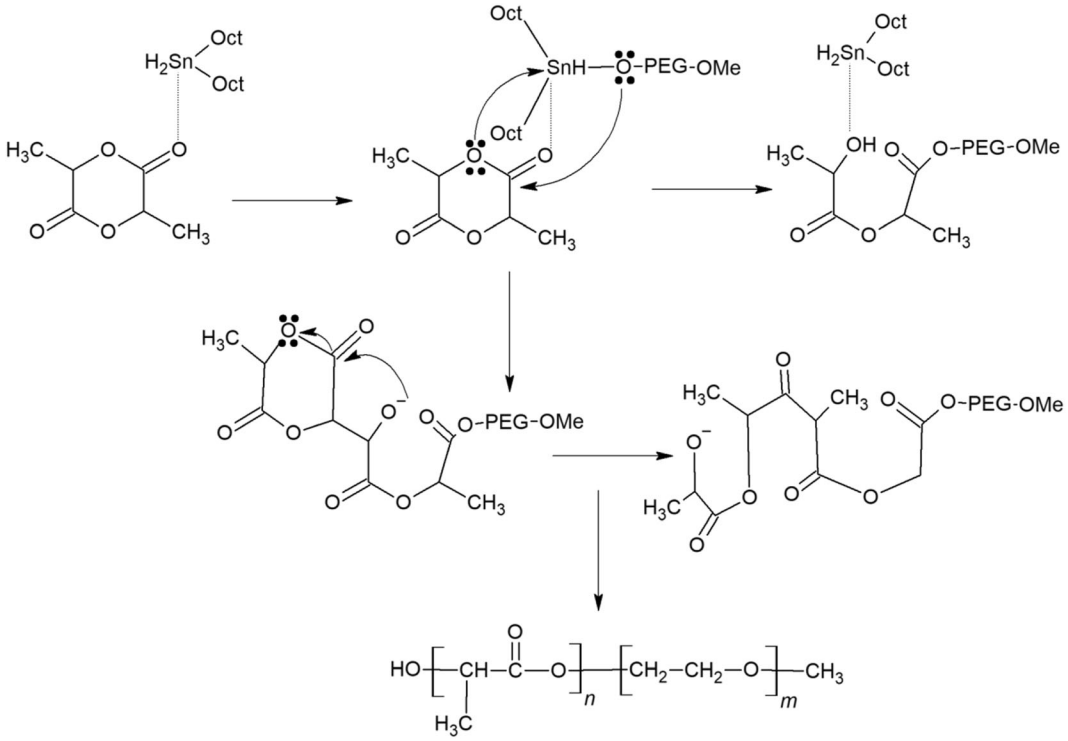


**Fig. 1.** Reaction mechanism for PLA-mPEG co-polymer formation for a ring-opening polymerization co-initiated by $Sn(Oct)_2$ and mPEG

method. PEI and herring sperm DNA complexes were formed at a DNA concentration of 0.08 mg/mL. The oil phase was comprised of PLA-mPEG polymer solution in DCM/EA and the PEI-DNA polyplexes. This phase was emulsified with the PVA solution ($W_1$) over a bed of dry ice for 10 s using a 3-mm ultrasonic probe (Sonics & Materials Inc., CT, USA) at a power output of 50 W. This solution was then placed into a syringe and stabilized with a 1% *w*/*v* PVA/sucrose solution in a second syringe (Fig. 2). These droplets were added to the second water phase with PVA at 38°C using a water bath and a heated magnetic stir plate (Fig. 2). The secondary emulsion was homogenized at 7500 rpm for 1 min. The solution was allowed to harden under constant stirring for 3 h. The resultant microparticles were centrifuged at 29×*g* in an Eppendorf Centrifuge 5804 R (Eppendorf, Westbury, NY) for 5 min and washed thrice with distilled water prior to analysis.

## Microparticle Characterization

The surface morphology of the particles and the primary particle size were obtained using scanning electron microscopy (SEM, Hitachi S-4000, Tokyo, Japan). SEM samples were prepared by dispersing microspheres in distilled water and adding to glass slides, allowing to dry and treating with osmium tetroxide overnight. Glass slides were mounted on metal stubs using double-sided carbon tape and vacuum coated with a thin layer (~5 nm) of gold by ion beam evaporation. Images were taken at 5 kV accelerating voltage, and the ImageJ software was used to manually determine the individual particle sizes (35).

Aerodynamic diameters of microspheres were estimated using time-of-flight analysis with an aerodynamic particle sizer (APS 3321, TSI, USA). Microspheres were allowed to air-dry on glass slides and dispersed into the aerosol flow path of the chamber, whereby individual particles were sized according to

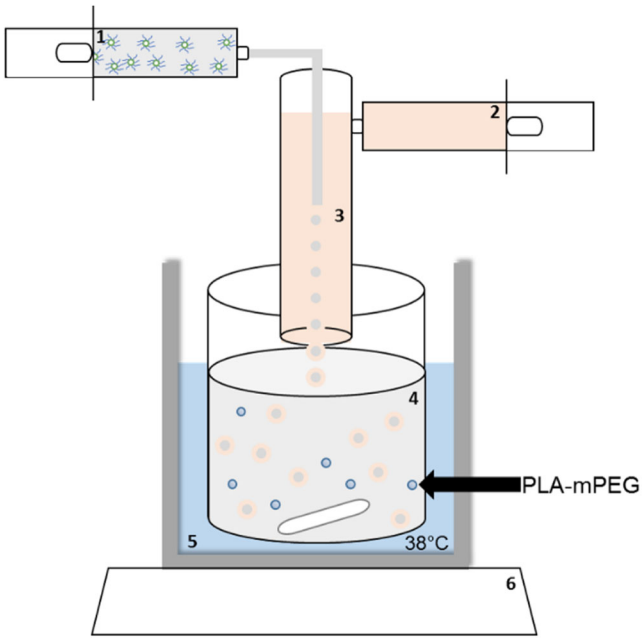


**Fig. 2.** Schematic representation of microparticle preparation. Two syringes were used to prepare particles, the first syringe (1) contained the oil phase of the emulsion, including the polymer and the polyplexes dissolved in DCM. The second syringe (2) was used to stabilize the droplets and contained a 1% (*w*/*v*) PVA solution. Initial droplets formed at the outlet of syringe 1 (3) and were added to the variable water phase in a beaker (4). The system was maintained in a water bath at 38°C (5), and stirred on a magnetic stir plate (6)

their transit time through two overlapping laser-diode beams. Each test consisted of aerosolizing three samples for 30 s with aerosol concentrations that ranged from 25 to 200 $cm^3$ as measured by the APS in summing mode. Aerodynamic size distributions and mean diameter were constructed using built-in software. The particle diameter corresponding with each peak (mode) in the APS output was determined using MATLAB find peaks function. Peaks were organized in order of decreasing intensity (frequency) and the top four modes for each formulation has been reported.

Encapsulation efficiency (*EE*) of PEI-DNA in microspheres was calculated using UV absorbance measurements at 260 nm (A260) (SpectraMax Plus$^{384}$ Microplate Spectrophotometer, Molecular Device) according to the following equation:

$$EE\,(\%) = \frac{\left(A260_{\text{initial}} - A260_{\text{supernatant}}\right)}{A260_{\text{initial}}} \times 100\% \quad (3)$$

The total amount of encapsulated DNA was calculated by measuring the amount of DNA left in the supernatant during the centrifugation and washing steps of the particle preparation. Supernatant samples were placed in quartz cuvettes and the absorbance was measured. Standard curves were obtained using a 2% *w/v* PVA solution with varying concentrations of PEI-DNA polyplexes from 1 to 100 μg/mL.

The *in vitro* release profile of the polyplexes from the porous microspheres was determined by incubating 10 mg/mL of PLA-mPEG particles in PBS in a 7-mL scintillation vial on a rotating shaker at 100 cycles/min and 37°C. Periodically, 1 mL of supernatant was removed from the scintillation vial and was replaced with an equivalent amount of PBS. This supernatant was centrifuged and analyzed in triplicate in a UV spectrophotometer at A260 to determine the DNA content.

## RESULTS

### Polymerization Characterization

Successful polymerization of PLA and mPEG was confirmed using $^1$H NMR spectroscopy (Figure S1). The chemical peak shifts were matched against literature values (Table I) and the area under the curves were used to determine the degree of polymerization and the number average molecular weight of the co-polymer mathematically as described in Eqs. 1–2. The degree of polymerization was determined from the calculated ratios of peak height for lactide in PLA (5.19 ppm) to ethylene glycol in mPEG (4–5 ppm). These ratios were consistent with the feed ratio, indicating that complete polymerization had occurred. Additionally, the absence of peaks at locations indicative of the monomers was used to confirm complete polymerization or sufficient washing. Although several formulations were prepared, only the PLA-mPEG co-polymer with number average molecular weight of 23 kDa was used for microparticle preparation.

**Table I.** Expected NMR Peak Shifts for the PLA-mPEG Co-Polymer and the Monomer Units

| Peak location (ppm) | Respective group |
|---|---|
| 5.19 | Lactide backbone |
| 3.65 | Ethylene oxide protons |
| 3–4 | Terminal methyl group, PEG |
| 1.6–1.7 | Unreacted lactide monomers |
| 5.0–5.1 | Unreacted lactide monomers |
| 2.85 | Unreacted mPEG monomers |
| 1.7 | Methyl group, PLA |
| 5.1 | Unreacted lactide or ethylene oxide backbone |

### Particle Porosity and Aerodynamic Diameter

Although the average diameter of particles is important, the aerodynamic diameter is more important because ultimately that will influence the degree of deposition in the target region. The aerodynamic diameter is dependent on the relationship between the particle size and density, and was measured using APS for each of the parameters investigated. In all cases, the particles had aerodynamic diameter distributions with multiple peaks, or modes, which indicate that the particles existed in many regions. Table II highlights the four most prominent modes for each formulation as measured with the APS. Even so, the region of interest is from 1 to 5 μm. The range of aerodynamic diameters decreased with increasing DP (dispersed phase, DCM/EA)/CP (continuous phase, PVA/sucrose) as did the number of observed modes (Figure S5). Only the 1% DP/CP had a large proportion of particles in the desired range. The greatest mode was at approximately 9 μm when the DP/CP was 10% (*v/v*). This maximum overlapped with the maxima for both DP/CP ratios of 1% *v/v* (10 μm) and 2% *v/v* (7 μm). However, each of the lower ratios had more modes, indicating more diverse sample sizes. Interestingly, none of the other parameters affected the number of modes present, although all ranges were affected. In particular, increasing the percentage of EA resulted in a narrower range, most notably at 50% EA (Figure S6). Additionally, at the same concentration, a large frequency peak developed in the desired size range. Overall, altering PVA was the most efficient method to obtain particles with modes in the desired range (Figure S7). Every concentration of PVA had a mode in the desired range, and both 0% *w/v* PVA and 5% *w/v* PVA had large modes within this range. Varying the amount of internal water in the emulsion (Figure S6) resulted in broader size distributions with greater amounts of internal water. Additionally, although the number of modes remained constant, the location of these modes shifted to larger diameters with increasing amounts of water. Taken together, these data indicate that many formulation methods can be utilized to develop respirable gene-loaded particles.

The presence of pores was confirmed using SEM micrographs (Fig. 3), and the primary particle size was recorded using ImageJ (Table III). The results show that porosity can be altered using any of the four parameters that were chosen, but there is a differing degree of effectiveness in increasing porosity and maintaining the spherical morphology. Furthermore, comparing the primary particle size (Table III) and the aerodynamic particle size (Table II) highlights the effects of porosity on aerodynamic diameter.

### Polyplex Loading and Release from Polymeric Microparticles

To ensure that the alterations in size and porosity did not compromise the loading or encapsulation efficiency of the

**Table II.** Aerodynamic Particle Sizes of Microspheres. Modes Were Determined From the Maximum Values in the Data Set. N/A Indicates That No Peaks Were Located. N/M Indicates That This Condition Was Not Measured with the APS. Italicized Numbers in Each Column Refer to the Line Items in Which the Parameter Was Treated as the Variable in the Experiments Where All Other Values Were Held Constant

| %DP/CP (*v/v*) | %EA (*v/v*) | %PVA (*w/v*) | %Water (% *v/v*) | %Polymer (*w/v*) | Mode 1 (μm) | Mode 2 (μm) | Mode 3 (μm) | Mode 4 (μm) |
|---|---|---|---|---|---|---|---|---|
| *1* | 7 | 2 | 5 | 5 | 10.19 | 1.24 | 19.92 | 4.85 |
| *2.5* | 7 | 2 | 5 | 5 | 6.97 | 15.09 | 20.05 | 24.35 |
| *5* | 7 | 2 | 5 | 5 | 15.35 | 20.15 | 10.26 | 5.15 |
| *10* | 7 | 2 | 5 | 5 | 10.18 | 17.76 | N/A | N/A |
| N/A | *0* | 2 | 5 | 5 | 15.44 | 20.33 | 9.99 | 3.72 |
| N/A | *15* | 2 | 5 | 5 | 7.13 | 12.81 | 19.09 | 3.34 |
| N/A | *25* | 2 | 5 | 5 | 5.68 | 14.96 | 11.02 | 21.07 |
| N/A | *50* | 2 | 5 | 5 | 3.00 | 6.17 | 10.64 | 12.05 |
| N/A | 7 | *0* | 5 | 5 | 5.28 | 10.20 | 15.08 | 22.75 |
| N/A | 7 | *3.5* | 5 | 5 | 7.34 | 10.47 | 5.02 | 15.26 |
| N/A | 7 | *5* | 5 | 5 | 4.02 | 8.26 | 12.64 | N/A |
| N/A | 7 | 2 | *3* | 5 | 10.76 | 5.80 | 15.84 | 20.08 |
| N/A | 7 | 2 | *10* | 5 | N/M | N/M | N/M | N/M |
| N/A | 7 | 2 | *20* | 5 | 30.97 | 20.32 | 42.72 | 14.80 |

polyplexes, we measured the DNA concentration using the absorbance at 260 nm. Encapsulation efficiency was determined by subtracting the remaining DNA in the supernatant after the washing steps and using Eq. 3. As the DP/CP increased, the encapsulation efficiency decreased (Table III). Overall, increasing the DP/CP from 1 to 10% decreased the

*Particle porosity and aerodynamic diameter*

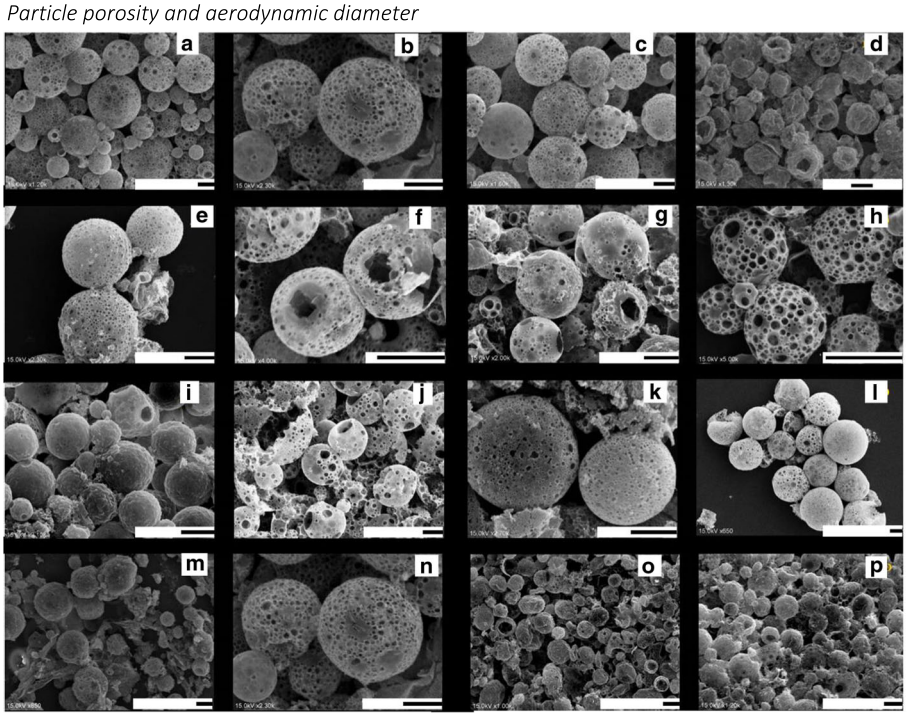


**Fig. 3.** SEM images of PLA-mPEG particles loaded with polyplexes. Each row represents one variable: DP/CP (top row), % EA (second row), % PVA (third row), % internal water (bottom row). Each individual image is representative of a different indicated treatment. The varying % DP/CP (*v/v*) includes 1% (**a**), 2% (**b**), 5% (**c**), and 10% (**d**) with constant PVA concentration (2% *w/v*), polymer concentration (5% *w/v*), EA concentration (7% *v/v*), and water concentration (5% *v/v*); the varying EA concentrations, include 0% (**e**), 15% (**f**), 25% (**g**), and 50% (**h**) with constant PVA concentration (2% *w/v*), polymer concentration (5% *w/v*), EA concentration (7% *v/v*), and water concentration (5% *v/v*). The varying internal water concentrations include 3% (**i**), 10% (**j**), 15% (**k**), and 20% (**l**), and constant PVA concentration (2% *w/v*), polymer concentration (5% *w/v*), and EA concentration (7% *v/v*). The varying internal PVA concentrations include 0% (**m**), 2% (**n**), 3.5% (**o**), and 5% (**p**) and constant PVA concentration (2% *w/v*), polymer concentration (5% *w/v*), EA concentration (7% *v/v*), and water concentration (5% *v/v*). The black scale bar represents 10 μm in each image

**Table III.** Microparticle Formulations and Corresponding Size Obtained From SEM Images and ImageJ, and Encapsulation Efficiency Calculated Using Absorbance Values and Eq. 3. Italicized Numbers in Each Column Refer to the Line Items in Which the Parameter Was Treated as the Variable in the Experiments Where All Other Values Were Held Constant

| %DP/CP (*v/v*) | %EA (*v/v*) | %PVA (*w/v*) | %Water (*v/v*) | %Polymer (*w/v*) | Average size (μm) | Encapsulation efficiency (%) |
|---|---|---|---|---|---|---|
| *1* | 7 | 2 | 5 | 5 | 13.4 ± 9.3 | 97.2 ± 2.30 |
| *2.5* | 7 | 2 | 5 | 5 | 13.4 ± 6.8 | 94.5 ± 1.18 |
| *5* | 7 | 2 | 5 | 5 | 13.4 ± 5.5 | 84.9 ± 0.94 |
| *10* | 7 | 2 | 5 | 5 | 10.9 ± 4.8 | 80.9 ± 4.85 |
| N/A | *0* | 2 | 5 | 5 | 12.6 ± 6.9 | 80.3 ± 0.637 |
| N/A | *15* | 2 | 5 | 5 | 11.2 ± 5.8 | 90.7 ± 2.47 |
| N/A | *25* | 2 | 5 | 5 | 12.2 ± 6.3 | 91.6 ± 2.72 |
| N/A | *50* | 2 | 5 | 5 | 6.6 ± 3.7 | 89.7 ± 1.23 |
| N/A | 7 | *0* | 5 | 5 | 10.5 ± 6.3 | 81.5 ± 1.98 |
| N/A | 7 | *3.5* | 5 | 5 | 8.8 ± 3.4 | 63.7 ± 6.36 |
| N/A | 7 | *5* | 5 | 5 | 7.6 ± 3.4 | 72.2 ± 6.95 |
| N/A | 7 | 2 | *3* | 5 | 9.4 ± 4.1 | 85.1 ± 1.08 |
| N/A | 7 | 2 | *10* | 5 | 14.0 ± 7.0 | 80.7 ± 8.26 |
| N/A | 7 | 2 | *20* | 5 | 27.4 ± 10.9 | 73.5 ± 5.15 |

encapsulation efficiency from 97 to 81%. Altering the internal water concentration also affected the encapsulation efficiency (Table III) to a greater extent than the DP/CP did. Specifically, encapsulation efficiency decreased from 85 to 74% over the concentration increase from 3 to 20%, respectively. Notably, the maximum encapsulation efficiency is quite low in comparison to the DP/CP results. Increasing the percentage of EA did not have any effect on the encapsulation efficiency at or above 15%, at which point all encapsulation efficiencies were approximately 90% (Table III). The encapsulation efficiency did not follow a clear trend with increasing the percentage of PVA (Table III). The maximum encapsulation efficiency observed was 85%, whereas the minimum was 78% (Table 3).

Using a similar method, the release of DNA was monitored over 15 days for each of the formulations (Figs. S2–S4). The release rate slowed with increasing DP/CP (Figure S2); almost 100% release was achieved after 350 h (14.6 days) at 10% DP/CP and after 250 h (10.4 days) at 5% DP/CP. With a constant DP/CP of 5%, increasing the percentage of water in the internal phase did not significantly alter the release profile (Figure S3). Additionally, increasing the water concentration appeared to decrease the release rate slightly up to 15% internal water (*v/v*); however, 20% water (*v/v*) in the internal phase had the fastest release. Compared with the previous two parameters, release rates for all percentages of PVA were much slower and only about 90% of the total polyplexes was released over 350 h (Figure S4). Additionally, each of the preparation conditions showed little to no release in the first 75 h of incubation indicating a delayed release profile.

## DISCUSSION

In an effort to generate a viable inhalable gene delivery system providing sustained-release kinetics, we have successfully fabricated polyplex-loaded microparticles with respirable aerodynamic diameters. PLA-mPEG co-polymers (23 kDa) were fabricated and used to encapsulate PEI-herring sperm DNA polyplexes using a double emulsion solvent evaporation method. The resultant microparticles were porous, had high encapsulation efficiency, and released the polyplexes over 10–15 days.

PLA-mPEG co-polymers have been used for drug delivery systems (36,37), and individually, PLA and PEG are both popular polymers for biological applications (38). PLA is a hydrophobic polymer commonly used in the pharmaceutical and biotechnology industries due to its low toxicity, biodegradability, and slow release *in vivo* (39). In the early 1970s, PLA was first used for biomedical applications in sutures and prosthetics (40), and then as a drug delivery agent for anti-narcotic treatment (41,42). PEG, a hydrophilic biocompatible polymer, is widely used in biomedical applications and can be used to extend resident times in the systemic circulation of encapsulated agents (43), and decrease toxicity caused by PEI (28,44). This latter property is particularly relevant to our application as it may aide in the biocompatibility of the PEI used in the formation of polyplexes. In order to determine the optimal co-polymer yield, the monomer feed ratio of PLA/mPEG has been previously investigated (45). This study utilized a set feed ratio of PLA/mPEG for the microspheres, which resulted in a high-yield PLA-mPEG co-polymers. The ratios of PLA to PEG in these co-polymers can be easily altered during polymer synthesis which in turn can affect the rate of polymer degradation and drug release (45).

In the present study, PLA-mPEG copolymers were formed using a ring-opening polymerization reaction catalyzed by $Sn(Oct)_2$. $Sn(Oct)_2$ is a commercially available catalyst that is soluble in many organic solvents, and reacts with lactide monomers within minutes to hours at temperatures ranging from 140 to 180°C (46). Additionally, $Sn(Oct)_2$ does not contain toxic groups, and therefore is safe for biological applications (47). The polymerization reaction is initiated *via* coordination-insertion, which limits the attachment of $Sn(Oct)_2$ as an end group (48). This, in turn, limits the attachment of Sn, thereby preventing its integration into the polymer. Successful polymerization and the resultant molecular weight of the polymers was obtained using $^1H$ NMR spectroscopy (Figure S1, Table I). This confirmed full esterification of mPEG after the polymerization reaction. The chemical shifts characteristic of the lactide

backbone (-O-CH($CH_3$)-CO) and the ethylene oxide protons (-O-$CH_2$-$CH_2$) were present at 5.19 and 3.65 ppm, respectively (49,50). An additional peak which can be attributed to the terminal methyl group in mPEG appeared next to the ethylene oxide peaks in the region of 3–4 ppm (51). The peaks for unreacted monomers were expected to appear at 1.6–1.7 ppm, 5.0–5.1 ppm for lactide monomers, and 2.85 ppm for mPEG monomers (49). However, one of these peaks for lactide overlapped with the expected peak for the methyl group in PLA at 1.7 ppm (52). There was a small peak at 5.1 ppm, which may have been unreacted lactide; however, the conversion ratio suggests full polymerization and therefore this was likely part of the ethylene oxide backbone rather than unreacted monomer. There was no peak for unreacted mPEG.

Polyester-based microparticles easily degrade into biological components *via* hydrolysis and therefore have been used to encapsulate plasmid DNA (pDNA) and other DNA moieties such as CpG oligodeoxynucleotides (CpG-ODN) (53–57). The precise amount of genetic material necessary to elicit the desired response varies based on disease, deposition, and release. Uchida et al. discovered that large amounts of pDNA were necessary to elicit gene expression from PEG-polycation-DNA complexes *in vitro* (20), and therefore, many studies focus solely on improving loading capacity rather than reaching a theoretical target. As expected, increasing the percentage *v/v* DP/CP resulted in decreased encapsulation efficiency (Table II) (58). Increasing the percentage of EA by up to 15% *v/v* corresponded to increased encapsulation efficiency (Table III). In contrast, increasing the percentage of internal water was expected to have the opposite effect because droplets would remain in the aqueous phase longer. Thus, encapsulation efficiency decreased with increasing the percentage of internal water (Table III). We suspect that utilizing a complex mixture of DCM/EA in the oil phase and PVA/sucrose in the water phase resulted in one of the solution components influencing outcomes such that we did not observe exactly the same trends that have been previously reported for less complex solutions. In a separate study, nanoparticles of PLGA-PEI were specifically prepared with the intention of pulmonary gene delivery (59). These nanoparticles were formulated with Poloxamer 188, rather than PVA, in the water phase, and the loading efficiencies were all at least 99%. In comparison, in our study, the encapsulation efficiency did not follow a clear trend in relation to PVA concentration, and altering the PVA did not result in encapsulation efficiencies even as high as 90% (Table III). We have previously reported that preparing polyplexes of PEI-pDNA prior to encapsulating into PLGA microparticles provides high loading efficiency (60), which was also observed in the present study with herring sperm DNA and PLA-mPEG microparticles in which the minimum encapsulation efficiency 74% (Table III).

For this study, we were concerned with how likely it was that the particles would deposit in the respiratory regions for gene delivery applications. As such, the aerodynamic particle size, which is a function of particle diameter and particle density, was measured with APS and used as a guide. Among all of the particle characteristics, the aerodynamic diameter is one of the most important because it will influence the degree of deposition in the target region. It is desirable to keep the aerodynamic diameter below 3 μm for efficient delivery to the airways (30). There is evidence that particles less than 1 μm are most likely to deposit in the alveoli, but are often exhaled prior to deposition (61). In many individuals using inhaler delivery systems, the ability for large particles (≥ 5 μm) to distribute throughout the lungs is very limited (62). In the present study, size distributions obtained from SEM and ImageJ were well outside the range of 3 μm, with the lowest average particle size of 9.4 μm at 3% internal water (Table III). However, greater degrees of porosity decrease the aerodynamic particle size and therefore highly porous particles were expected to have the best modes in the desired size range. Fifty percent EA appeared to have the greatest pore volume qualitatively (Fig. 3h), and the corresponding APS distribution indeed had a large mode in the desired size range as well as the smallest range of aerodynamic diameters (Figure S6). Increasing the amount of PVA also had a positive effect on the APS distribution in which larger concentrations resulted in larger modes in the desired size range and a more narrow size distribution (Figure S7). Increasing the percentage of DP/CP decreased the number of modes and the range; however, it did not increase the intensity of the mode within the desired size range. Thus, this parameter had the lowest effect on the aerodynamic diameter for the desired applications.

One of the key drawbacks in inhaled gene therapy is the inability to load optimal therapeutic amounts of necessary genes. Although this was not addressed directly in this manuscript, achieving high encapsulation efficiencies of the polyplexes is promising in terms of delivering potentially effective DNA doses. Furthermore, greater encapsulation efficiency tends to correspond to slower drug release rates due to diffusivity (63). This is particularly advantageous for long-term treatment methods, particularly those requiring repeated administration. As such, a summary of the parameters which produced microparticles with the highest encapsulation efficiencies is presented in Table IV. Developing particles that reliably deposit within the lungs according to respiratory deposition models (1–3 μm aerodynamic diameters) improves the likelihood that the genes will be released at

**Table IV.** Formulation Parameters Resulting in the Highest Encapsulation Efficiency for Each Variable. The Parameter Marked with an Asterisk (*) in Each Column Denotes the Variable That Was Changed for Those Particular Studies. N.D. Indicates No Data as the Parameter Was Not Calculated or Reported for These Conditions

| DP/CP (%) | EA (%) | Internal water concentration (%) | Internal PVA concentration (%) | Average size (μm) | Encapsulation efficiency (%) |
|---|---|---|---|---|---|
| 1* | 7 | 5 | 2 | 13.4 ± 5.5 | 97.2 ± 2.3 |
| N.D. | 25* | 5 | 2 | 12.2 ± 6.3 | 91.6 ± 2.8 |
| N.D. | 7 | 3* | 2 | 9.40 ± 4.1 | 85.1 ± 1.1 |
| N.D. | 7 | 5 | 1.25* | 14.0 ± 6.6 | 85.7 ± 6.0 |

the target location. The delayed release of genes for over 72 h (3 days) is potentially a disadvantage if treatment needs to begin immediately. On the other hand, mitigating burst release ensures that more of the cargo is present in the microsphere for longer times.

## CONCLUSIONS AND FUTURE DIRECTIONS

DNA loading into microparticles was increased only with increasing the percentage of EA (*v*/*v*) in the oil phase; however, it did ultimately plateau. Encapsulation efficiency is crucial for gene delivery formulations since the gene must be present in sufficient quantities to be effective. Increasing DP/CP, percentage of EA, and percentage of PVA shifted the modes and range of the aerodynamic diameter to smaller sizes. All release profiles showed that most of the herring sperm DNA was released within 15 days; therefore, this formulation has a lifetime of approximately 2 weeks.

When considering the clinical translational ability of these formulations, one must also consider the toxicity imposed by the particles. The mechanism of polymerization is favorable such that no toxic products were used and all unreacted monomers were removed from the system during purification. Furthermore, although PEI has been shown to cause systemic toxicity at high concentrations, PEG is effective at mitigating this toxicity. Future studies will need to include toxicity studies *in vitro* and *in vivo* to confirm this.

## ACKNOWLEDGEMENTS

The authors would like to acknowledge Terra M. Kruger for help with the NMR spectra, and Prof. Kristan S. Worthington for assistance with the polymerization reaction. The SEM images were obtained using an SEM instrument in the Central Microscopy Research Facilities at The University of Iowa.

## FUNDING INFORMATION

A.K.S acknowledges support from the NIH P30 CA086862 grant and the Lyle and Sharon Bighley Chair of Pharmaceutical Sciences. T.L.T. acknowledges support from the Department of Education GAANN Fellowship program. B.E.G. acknowledges funding support from the Alfred P. Sloan Foundation, the University of Iowa Graduate College, and the National GEM Consortium. V. G. J. R. acknowledges support from the Jacques S. Yeager, Sr. endowment.

## COMPLIANCE WITH ETHICAL STANDARDS

**Conflict of Interest** The authors declare that they have no conflict of interest.

**Publisher's note** Springer Nature remains neutral with regard to jurisdictional claims in published maps and institutional affiliations.

## REFERENCES

1. Jacobson SG, Cideciyan AV, Roman AJ, Sumaroka A, Schwartz SB, Heon E, et al. Improvement and decline in vision with gene therapy in childhood blindness. N Engl J Med. 2015;372(20):1920–6.
2. Finotti A, Breda L, Lederer CW, Bianchi N, Zuccato C, Kleanthous M, et al. Recent trends in the gene therapy of beta-thalassemia. J Blood Med. 2015;6:69–85.
3. Villate-Beitia I, Zarate J, Puras G, Pedraz JL. Gene delivery to the lungs: pulmonary gene therapy for cystic fibrosis. Drug Dev Ind Pharm. 2017;43(7):1071–81.
4. Griesenbach U, Pytel KM, Alton EW. Cystic fibrosis gene therapy in the UK and elsewhere. Hum Gene Ther. 2015;26(5):266–75.
5. Sabatel C, Radermecker C, Fievez L, Paulissen G, Chakarov S, Fernandes C, et al. Exposure to bacterial CpG DNA protects from airway allergic inflammation by expanding regulatory lung interstitial macrophages. Immunity. 2017;46(3):457–73.
6. Olin JT, Wechsler ME. Asthma: pathogenesis and novel drugs for treatment. BMJ. 2014;349(7):g5517.
7. Gomes Dos Reis L, Svolos M, Hartwig B, Windhab N, Young PM, Traini D. Inhaled gene delivery: a formulation and delivery approach. Expert Opin Drug Deliv. 2017;14(3):319–30.
8. Shalash AO, Khalafallah NM, Molokhia AM, Elsayed MMA. The relationship between the permeability and the performance of carrier-based dry powder inhalation mixtures: new insights and practical guidance. AAPS PharmSciTech. 2018;19(2):912–22.
9. Sheth P, Stein SW, Myrdal PB. Factors influencing aerodynamic particle size distribution of suspension pressurized metered dose inhalers. AAPS PharmSciTech. 2015;16(1):192–201.
10. Singh B, Bandopadhyay S, Kapil R, Singh R, Katare O. Self-emulsifying drug delivery systems (SEDDS): formulation development, characterization, and applications. Crit Rev Ther Drug Carrier Syst. 2009;26(5):427–521.
11. Morales JO, Fathe KR, Brunaugh A, Ferrati S, Li S, Montenegro-Nicolini M, et al. Challenges and future prospects for the delivery of biologics: oral mucosal, pulmonary, and transdermal routes. AAPS J. 2017;19(3):652–68.
12. Liechty WB, Kryscio DR, Slaughter BV, Peppas NA. Polymers for drug delivery systems. Annu Rev Chem Biomol Eng. 2010;1:149–73.
13. Kleemann E, Jekel N, Dailey LA, Roesler S, Fink L, Weissmann N, et al. Enhanced gene expression and reduced toxicity in mice using polyplexes of low-molecular-weight poly(ethylene imine) for pulmonary gene delivery. J Drug Target. 2009;17(8):638–51.
14. Ebeid K, Meng X, Thiel KW, Do AV, Geary SM, Morris AS, et al. Synthetically lethal nanoparticles for treatment of endometrial cancer. Nat Nanotechnol. 2018;13(1):72–81.
15. Do AV, Geary SM, Seol D, Tobias P, Carlsen D, Leelakanok N, et al. Combining ultrasound and intratumoral administration of doxorubicin-loaded microspheres to enhance tumor cell killing. Int J Pharm. 2018;539(1–2):139–46.
16. Wongrakpanich A, Morris AS, Geary SM, Joiner MA, Salem AK. Surface-modified particles loaded with CaMKII inhibitor protect cardiac cells against mitochondrial injury. Int J Pharm. 2017;520(1–2):275–83.
17. Wafa EI, Geary SM, Goodman JT, Narasimhan B, Salem AK. The effect of polyanhydride chemistry in particle-based cancer vaccines on the magnitude of the anti-tumor immune response. Acta Biomater. 2017;50:417–27.
18. Morris AS, Sebag SC, Paschke JD, Wongrakpanich A, Ebeid K, Anderson ME, et al. Cationic CaMKII inhibiting nanoparticles prevent allergic asthma. Mol Pharm. 2017;14(6):2166–75.
19. Ahmed KK, Geary SM, Salem AK. Surface engineering tumor cells with adjuvant-loaded particles for use as cancer vaccines. J Control Release. 2017;248:1–9.
20. Uchida S, Itaka K, Chen Q, Osada K, Ishii T, Shibata MA, et al. PEGylated polyplex with optimized PEG shielding enhances gene introduction in lungs by minimizing inflammatory responses. Mol Ther. 2012;20(6):1196–203.
21. Laube BL. The expanding role of aerosols in systemic drug delivery, gene therapy, and vaccination. Respir Care. 2005;50(9):1161–76.
22. Al-Dosari MS, Gao X. Nonviral gene delivery: principle, limitations, and recent progress. AAPS J. 2009;11(4):671–81.
23. Intra J, Salem AK. Fabrication, characterization and in vitro evaluation of poly(D,L-lactide-co-glycolide) microparticles loaded with polyamidoamine-plasmid DNA dendriplexes for applications in nonviral gene delivery. J Pharm Sci. 2010;99(1):368–84.

24. Abbas AO, Donovan MD, Salem AK. Formulating poly(lactide-co-glycolide) particles for plasmid DNA delivery. J Pharm Sci. 2008;97(7):2448–61.
25. Zhang XQ, Intra J, Salem AK. Conjugation of polyamidoamine dendrimers on biodegradable microparticles for nonviral gene delivery. Bioconjug Chem. 2007;18(6):2068–76.
26. Zhang XQ, Dahle CE, Baman NK, Rich N, Weiner GJ, Salem AK. Potent antigen-specific immune responses stimulated by codelivery of CpG ODN and antigens in degradable microparticles. J Immunother. 2007;30(5):469–78.
27. Intra J, Salem AK. Characterization of the transgene expression generated by branched and linear polyethylenimine-plasmid DNA nanoparticles in vitro and after intraperitoneal injection in vivo. J Control Release. 2008;130(2):129–38.
28. Kim N, Jiang D, Jacobi AM, Lennox KA, Rose SD, Behlke MA, et al. Synthesis and characterization of mannosylated pegylated polyethylenimine as a carrier for siRNA. Int J Pharm. 2012;427(1):123–33.
29. Jiang D, Salem AK. Optimized dextran-polyethylenimine conjugates are efficient non-viral vectors with reduced cytotoxicity when used in serum containing environments. Int J Pharm. 2012;427(1):71–9.
30. Edwards DA, Hanes J, Caponetti G, Hrkach J, Ben-Jebria A, Eskew ML, et al. Large porous particles for pulmonary drug delivery. Science. 1997;276(5320):1868–71.
31. Klassen CD, Watkins JBI. Casarett & Doull's essentials of toxicology. 2nd ed: McGraw-Hill Education / Medical; 2015. 528 p
32. Kamada Ltd. International study evaluating the safety and efficacy of inhaled, human, alpha-1 antitrypsin (AAT) in alpha-1 antitrypsin deficient patients with emphysema. 2014.
33. Duncan GA, Jung J, Hanes J, Suk JS. The mucus barrier to inhaled gene therapy. Mol Ther. 2016;24(12):2043–53.
34. Kim N, Duncan GA, Hanes J, Suk JS. Barriers to inhaled gene therapy of obstructive lung diseases: a review. J Control Release. 2016;240:465–88.
35. Abramoff MD, Magalhaes PJ, Ram SJ. Image processing with ImageJ. Biophoton Int. 2004;11(7):36–42.
36. Singh NA, Mandal AKA, Khan ZA. Fabrication of PLA-PEG nanoparticles as delivery systems for improved stability and controlled release of catechin. J Nanomater. 2017;2017:1–9.
37. Sakhalkar HS, Dalal MK, Salem AK, Ansari R, Fu J, Kiani MF, et al. Leukocyte-inspired biodegradable particles that selectively and avidly adhere to inflamed endothelium in vitro and in vivo. Proc Natl Acad Sci U S A. 2003;100(26):15895–900.
38. Sinclair J, Salem AK. Rapid localized cell trapping on biodegradable polymers using cell surface derivatization and microfluidic networking. Biomaterials. 2006;27(9):2090–4.
39. Jain A, Kunduru KR, Basu A, Mizrahi B, Domb AJ, Khan W. Injectable formulations of poly(lactic acid) and its copolymers in clinical use. Adv Drug Deliv Rev. 2016;107:213–27.
40. Kulkarni RK, Moore EG, Hegyeli AF, Leonard F. Biodegradable poly(lactic acid) polymers. J Biomed Mater Res. 1971;5(3):169–81.
41. Woodland JH, Yolles S, Blake DA, Helrich M, Meyer FJ. Long-acting delivery systems for narcotic antagonists. 1. J Med Chem. 1973;16(8):897–901.
42. Yolles S, Leafe TD, Woodland JH, Meyer FJ. Long acting delivery systems for narcotic antagonists II: release rates of naltrexone from poly(lactic acid) composites. J Pharm Sci. 1975;64(2):348–9.
43. Vila A, Sanchez A, Evora C, Soriano I, McCallion O, Alonso MJ. PLA-PEG particles as nasal protein carriers: the influence of the particle size. Int J Pharm. 2005;292(1–2):43–52.
44. Lu S, Morris VB, Labhasetwar V. Codelivery of DNA and siRNA via arginine-rich PEI-based polyplexes. Mol Pharm. 2015;12(2):621–9.
45. Zhu KJ, Lin XZ, Yang SL. Preparation, characterization, and properties of polylactide (Pla) poly(ethylene glycol) (peg) copolymers - a potential-drug carrier. J Appl Polym Sci. 1990;39(1):1–9.
46. Dechy-Cabaret O, Martin-Vaca B, Bourissou D. Controlled ring-opening polymerization of lactide and glycolide. Chem Rev. 2004;104(12):6147–76.
47. Kricheldorf HR, Sumbel MV, Kreiser-Saunders I. Polylactones. 20. Polymerization of ιε-caprolactone with tributyltin derivatives: a mechanistic study. Macromolecules. 1991;24(8):1944–9.
48. Kricheldorf HR, Kreiser-Saunders I, Stricker A. Polylactones 48. SnOct2-initiated polymerizations of lactide: a mechanistic study. Macromolecules. 2000;33(3):702–9.
49. Beletsi A, Leontiadis L, Klepetsanis P, Ithakissios DS, Avgoustakis K. Effect of preparative variables on the properties of poly(dl-lactide-co-glycolide)-methoxypoly(ethyleneglycol) copolymers related to their application in controlled drug delivery. Int J Pharm. 1999;182(2):187–97.
50. Zheng X, Kan B, Gou M, Fu S, Zhang J, Men K, et al. Preparation of MPEG-PLA nanoparticle for honokiol delivery in vitro. Int J Pharm. 2010;386(1–2):262–7.
51. Alibolandi M, Sadeghi F, Sazmand SH, Shahrokhi SM, Seifi M, Hadizadeh F. Synthesis and self-assembly of biodegradable polyethylene glycol-poly (lactic acid) diblock copolymers as polymersomes for preparation of sustained release system of doxorubicin. Int J Pharm Investig. 2015;5(3):134–41.
52. Luo WJ, Li SM, Bei JZ, Wang SG. Synthesis and characterization of poly(L-lactide)- poly(ethylene glycol) multiblock copolymers. J Appl Polym Sci. 2002;84(9):1729–36.
53. Vert M. Degradable polymers in medicine: updating strategies and terminology. Int J Artif Organs. 2011;34(2):76–83.
54. Salem AK, Weiner GJ. CpG oligonucleotides as immunotherapeutic adjuvants: innovative applications and delivery strategies. Adv Drug Deliv Rev. 2009;61(3):193–4.
55. Krishnamachari Y, Salem AK. Innovative strategies for co-delivering antigens and CpG oligonucleotides. Adv Drug Deliv Rev. 2009;61(3):205–17.
56. Joshi VB, Adamcakova-Dodd A, Jing X, Wongrakpanich A, Gibson-Corley KN, Thorne PS, et al. Development of a poly (lactic-co-glycolic acid) particle vaccine to protect against house dust mite induced allergy. AAPS J. 2014;16(5):975–85.
57. Makkouk A, Joshi VB, Wongrakpanich A, Lemke CD, Gross BP, Salem AK, et al. Biodegradable microparticles loaded with doxorubicin and CpG ODN for in situ immunization against cancer. AAPS J. 2015;17(1):184–93.
58. Hsu YY, Hao T, Hedley ML. Comparison of process parameters for microencapsulation of plasmid DNA in poly(D,L-lactic-co-glycolic) acid microspheres. J Drug Target. 1999;7(4):313–23.
59. Bivas-Benita M, Romeijn S, Junginger HE, Borchard G. PLGA-PEI nanoparticles for gene delivery to pulmonary epithelium. Eur J Pharm Biopharm. 2004;58(1):1–6.
60. Zhang XQ, Intra J, Salem AK. Comparative study of poly (lactic-co-glycolic acid)-poly ethyleneimine-plasmid DNA microparticles prepared using double emulsion methods. J Microencapsul. 2008;25(1):1–12.
61. Bailey MM, Berkland CJ. Nanoparticle formulations in pulmonary drug delivery. Med Res Rev. 2009;29(1):196–212.
62. Biddiscombe MF, Usmani OS. Inhaler characteristics in asthma. EU Respir Pulm Dis. 2017;3:32–7.
63. Huang YY, Chung TW, Tzeng TW. Drug release from PLA/PEG microparticulates. Int J Pharm. 1997;156(1):9–15.